

Simulation of Blood Flow in the Left Ventricle Considering Purkinje Fibers

Misaki Iwai¹[0009-0003-6650-2572], Yusuke Nishiya¹, Masashi Yamakawa¹[0000-0001-5960-2602],
Ayato Takii²[0000-0003-3257-7640], Yusei Kobayashi¹[0000-0002-5690-2033], Takahiro Ikeda¹[0009-
0008-7496-9056], Shinichi Asao³[0000-0003-4326-8480] and Seiichi Takeuchi³

¹Kyoto Institute of Technology, Matsugasaki, Sakyo-ku, Kyoto 606-8585, Japan
m4623004@kit.edu.ac.jp

² Kobe University, Rokkodai, Nsda-ku, Kobe, Hyogo 657-8501, Japan

³ College of Industrial Technology, 1-27-1, Amagasaki, Hyogo 661-0047, Japan

Abstract. Heart disease is the leading cause of death worldwide. To determine the factors contributing to the development of cardiac disease, computational fluid dynamics (CFD) and *in vivo* data, such as MRI of blood flow, are being compared and validated to better understand the hemodynamics of the heart in detail. The cardiac conduction system, which transmits electrical signals and controls the heart's beating, is also being studied. However, no studies have examined the relationship between the cardiac conduction system and left ventricular hemodynamics. In this study, we focused on the Purkinje fibers located in the left ventricle within the cardiac conduction system. The simulation results of left ventricular models with and without Purkinje fibers were compared. The results showed differences in blood flow within the left ventricle. Thus, changes in contraction caused by the Purkinje fibers affect the hemodynamics of the left ventricle and can contribute to the development of heart disease.

Keywords: CFD, Purkinje fiber, cardiac conduction system (CCS), left ventricular

1 Introduction

In the human body, blood is continuously circulated through blood vessels by the beating of the heart, playing a crucial role in sustaining life. As a result, heart diseases are often life-threatening. According to the WHO [1], ischemic heart disease was the leading cause of death worldwide for 18 consecutive years up to 2019. Even in 2021, when COVID-19 caused global disruption and became the second leading cause of death, ischemic heart disease remained the top cause.

A relationship between heart disease and blood flow has been suggested, and detailed understanding of cardiac hemodynamics has been utilized to explore the mechanisms of disease development. *In silico* studies, such as numerical simulations, are non-invasive and allow for intuitive flow visualization. In recent years, advanced imaging technologies such as *in vivo* CT and MRI have enabled the acquisition of detailed data on

the dynamic shape and motion of the heart. These data have been incorporated into simulations to perform calculations under physiologically realistic conditions. Many CFD studies [2-4] have focused on the left ventricle, which is particularly prone to cardiac diseases.

The cardiac conduction system (CCS), including the Purkinje fibers, generates and transmits electrical signals in cardiac muscle. There are two types of cardiac muscle: specialized cardiac muscle that transmits electrical impulses, and intrinsic cardiac muscle that contracts in response. Electrical signals generated by the sinus node are transmitted through the His bundle to the Purkinje fibers, which spread across the left ventricle [5]. Since the CCS governs the heart's rhythm, it plays a critical role in cardiac motion and should be considered in motion analysis. However, the relationship between CCS activity and heart function is difficult to investigate experimentally, and has thus been explored through simulations [6-7]. Previous studies have mainly focused on the resulting mechanical motion, rather than how the electrical stimulus propagation affects blood flow. Conventional CFD simulations often assume synchronous contraction across the left ventricular wall; however, actual contraction timing is dictated by the conduction sequence. Previous studies have mainly focused on the resulting mechanical motion, rather than how the propagation of electrical stimuli affects hemodynamics. Conventional CFD simulations often assume that both systole and diastole begin simultaneously across the entire left ventricular wall; however, in reality, their timing is governed by the conduction sequence. This study aims to clarify whether incorporating the CCS into blood flow simulations improves the reproducibility of left ventricular hemodynamics. To this end, simulations were conducted using two models—one with and one without the Purkinje network.

The unstructured moving grid finite volume method [8-9] is applied for calculations using the fractional step method, with the LU-SGS method [10] employed as the iterative method for the first step and the Bi-CGSTAB method [11] for the second step, as both are implicit solution methods. To accommodate complex movements such as valve opening and closing, ventricular systole and diastole, and torsion, a grid movement method that simulates the effect of a torsion spring is employed. Due to the increased computational cost, we aim to accelerate computations by utilizing OpenMP for parallel processing [12]. By considering whether Purkinje fibers contribute to the accuracy of blood flow reproduction, we hope to gain a more detailed understanding of hemodynamics and investigate heart diseases.

2 Numerical Approach

2.1 Governing Equation

Blood viscosity remains nearly constant regardless of hematocrit when the shear rate exceeds 100 s^{-1} (corresponding to a Reynolds number of several hundred). In the region from the left ventricle to the aortic arch, the Reynolds number exceeds 1000, making the assumption of Newtonian fluid behavior valid. Therefore, in this study, blood is treated as an incompressible Newtonian fluid, and the three-dimensional incompressible Navier-Stokes and continuity equations (1)-(3) are used as the governing equations.

Here, \mathbf{q} is the conserved quantity vector, and $\mathbf{E}, \mathbf{F}, \mathbf{G}$ are the inviscid flux vectors in the x, y, z directions, $\mathbf{E}_v, \mathbf{F}_v, \mathbf{G}_v$ are the viscous flux vectors in the same directions. In addition, u, v, w are velocity components, p is pressure, and Re is the Reynolds number. The subscripts x, y, z in the $\mathbf{E}_v, \mathbf{F}_v, \mathbf{G}_v$ components represent derivatives in each direction. Note that the above equations are expressed in dimensionless form.

$$\frac{\partial \mathbf{q}}{\partial t} + \frac{\partial \mathbf{E}}{\partial x} + \frac{\partial \mathbf{F}}{\partial y} + \frac{\partial \mathbf{G}}{\partial z} = \frac{1}{\text{Re}} \left(\frac{\partial \mathbf{E}_v}{\partial x} + \frac{\partial \mathbf{F}_v}{\partial y} + \frac{\partial \mathbf{G}_v}{\partial z} \right), \quad (1)$$

$$\mathbf{q} = \begin{bmatrix} u \\ v \\ w \end{bmatrix}, \quad \mathbf{E} = \begin{bmatrix} u^2 + p \\ uv \\ uw \end{bmatrix}, \quad \mathbf{F} = \begin{bmatrix} vu \\ v^2 + p \\ vw \end{bmatrix}, \quad \mathbf{G} = \begin{bmatrix} wu \\ wv \\ w^2 + p \end{bmatrix},$$

$$\mathbf{E}_v = \begin{bmatrix} u_x \\ v_x \\ w_x \end{bmatrix}, \quad \mathbf{F}_v = \begin{bmatrix} u_y \\ v_y \\ w_y \end{bmatrix}, \quad \mathbf{G}_v = \begin{bmatrix} u_z \\ v_z \\ w_z \end{bmatrix}, \quad (2)$$

$$\frac{\partial u}{\partial x} + \frac{\partial v}{\partial y} + \frac{\partial w}{\partial z} = 0. \quad (3)$$

2.2 The Unstructured Moving Grid Finite Volume Method

Pulsatile flow in the left ventricle presents a moving boundary problem, driven by time-varying wall geometry and requiring dynamic mesh deformation. To address this, the unstructured moving grid finite volume method [8-9] was employed. This method is well-suited for such problems, as it conserves physical quantities using space-time control volumes and strictly satisfies the geometric conservation law.

3 Computational model

3.1 Left Ventricular Pulsation Conditions

At a heart rate of 60 beats per minute, systole and diastole occupy approximately 0.49 and 0.51 seconds, respectively. During systole, efficient ejection is achieved primarily through coordinated wall motion, including wall thickening—which causes inward displacement of the endocardial surface—and torsional motion along the long axis. Of these mechanisms, the inward displacement due to wall thickening is indirectly reflected in the volume change, which follows the data presented in [13]. As for the torsional motion, according to [14], assuming normal physiological twisting, the torsional angle is defined as positive in the counterclockwise direction when viewed from the apex, with a maximum of $+3^\circ$ at the base and -7.8° at the apex.

3.2 Conditions for Conduction of Stimulation of the Left Ventricle

Stimulus conduction is calculated on a grid of the left ventricular wall with three patterns: (1) Purkinje to Purkinje (P–P), (2) Purkinje to intrinsic cardiac muscle (P–I), and (3) intrinsic cardiac muscle to intrinsic cardiac muscle (I–I). As shown in Fig. 1,

calculations are performed for each pattern individually. The conduction condition is determined based on the distance from the grid point where the stimulus originates, with radii R1 for (1) and R2 for (2) and (3). According to the literature [15-16], the ratio of conduction velocities is set to $R1:R2 = 10:1$. In this study, the conduction velocity of the intrinsic cardiac muscle is set to 0.1 cm/step, and that of the Purkinje fibers to 1.0 cm/step.

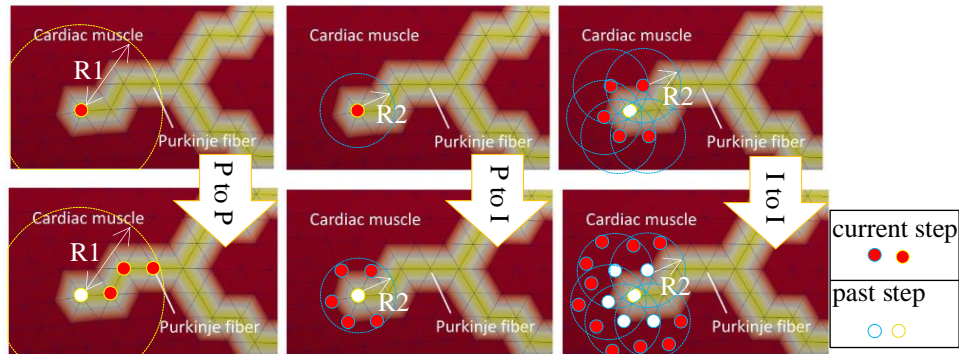


Fig. 1 Three patterns of stimulation conduction

3.3 Left Ventricle Model

The computational grid consists of tetrahedral elements in the interior and prismatic grids near the wall. The left ventricular model contains 1,145,432 elements (755,042 tetrahedral and 390,390 prismatic), and was generated using MEGG3D [17-18]. At maximum cavity volume, the vessel diameter at the mitral and aortic valves is 3.0 cm, and the distance from the cardiac base to the apex is 7.8 cm. The cross-section is elliptical, with an axial diameter ratio of 1.0:0.8.

According to theories of Purkinje fiber distribution, they first branch from the His bundle into the left anterior and posterior fascicles, which then fan out across the left ventricular wall. Two main branching patterns have been proposed: in one, fibers wrap around the left ventricular apex; in the other, they extend over the anterior and posterior walls after a slight downward turn of the fibers [7]. Based on these patterns, the grid points on the left ventricular wall were classified into specialized and intrinsic cardiac muscle types, as shown in Fig. 2, and modeled accordingly. While the terminal branches of Purkinje fibers form a fine mesh-like network in reality, significant individual variation exists, so a simplified representation is used in this study.

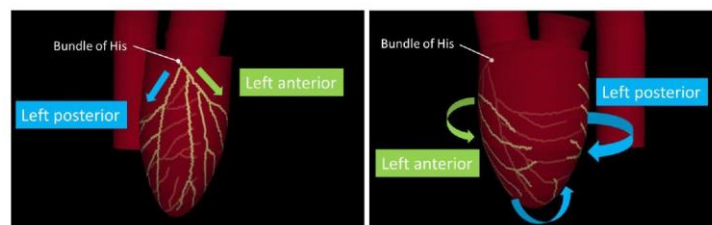


Fig. 2 Purkinje fiber distribution in this model

3.4 Calculation Conditions

Table 1 lists the characteristic values for this simulation.

Initial conditions are: pressure $p = 0.0$ and velocity $u = v = w = 0.0$ for all elements. The time increment is $\Delta t = 0.0005$, and the simulation begins in diastole and runs for three left ventricular beats.

Next, the boundary conditions are described. The left ventricular wall is assumed to be a no-slip wall during both systole and diastole.

- During diastole, the mitral valve is fully open and the aortic valve fully closed.
- During systole, the mitral valve is fully closed and the aortic valve fully open.
- At the open valve, velocity is applied according to a nonlinear function approximated from the graph shown in [20], and the pressure is fixed at $p = 0.0$.
- At wall surfaces including closed valves, the velocity matches that of the moving wall, and the pressure is given by Equation (4), accounting for acceleration of the wall motion α .
- The opening and closing of the mitral and aortic valves are assumed to occur instantaneously at the onset of diastole and systole.

$$\frac{\partial p}{\partial x} = -\alpha. \quad (4)$$

Table 1. Characteristic values

characteristic length (\bar{L}_0)	0.03 [m]	the vessel diameter at the aortic valve
characteristic kinematic viscosity coefficient ($\bar{\nu}_0$)	4.43×10^{-6} [m ² /s]	the value for blood
characteristic velocity (\bar{U}_0)	0.30 [m/s]	the average outflow velocity from the left ventricle during systole

4 Simulation Results

4.1 Validity of the Purkinje Model Results

Hereafter, the conventional model assumes uniform contraction of the entire left ventricle without accounting for electrical conduction, whereas the Purkinje model incorporates conduction dynamics into the contraction process. Figure 3 shows the stimulus transmission behavior. The yellow regions indicate areas where the electrical stimulus has been transmitted. The stimulus rapidly spreads throughout the left ventricle via the Purkinje fibers. The presence of these fibers enables rapid propagation to the apex. This apex-first activation is known to contribute to a squeezing motion, as suggested in literature [15,19].

Figure 4 shows streamlines during the third diastolic phase in both models. In both models, two asymmetric vortices are generated. The central vortex is larger, consistent with blood flow measurements by Kilner et al. [20]. The dynamics and energy of these

vortices have been analyzed in previous studies [21], supporting the validity of the Purkinje model for left ventricular flow simulation.

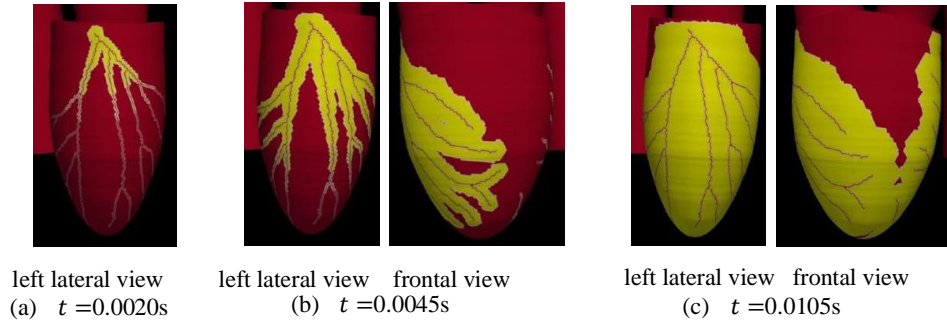


Fig. 3 The stimulus transmission behavior

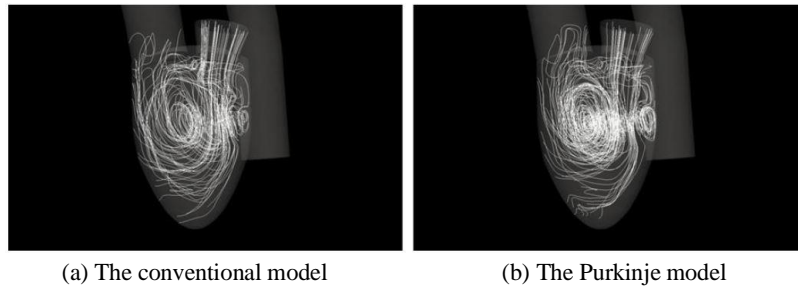


Fig. 4 The streamlines in both models

4.2 Differences Between the Purkinje Model and the Conventional Model

Iso-surfaces of the Q-values are commonly used to extract vortex structures. Figure 5 shows the differences in blood flow between the two models during the late systolic phase. The comparison reveals that slight differences in the motion of the left ventricular wall lead to minor variations in the flow field. These differences are particularly noticeable in the central region of the left ventricle. This is likely because the vortex described in Section 4.1 disturbs the surrounding flow, making the small differences in wall motion manifest as flow differences in the central area.

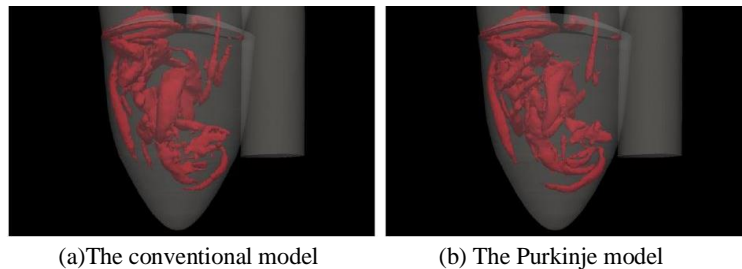


Fig. 5 Iso-surface visualization of the Q-values in the late systolic phase

5 Conclusions

This study is the first to incorporate Purkinje fibers into blood flow simulations. The objective was to investigate how the timing of left ventricular contraction, altered by stimulus conduction via Purkinje fibers, affects intraventricular blood flow behavior. By comparing simulation results with and without stimulus conduction, the following conclusions were drawn:

- The results of stimulus conduction using a Purkinje fiber model in the left ventricular wall were consistent with clinical data, confirming the validity of the Purkinje fiber distribution and conduction mechanism.
- Visualization of streamlines revealed the formation of asymmetric vortices in the central region and near the wall of the left ventricle. The characteristics of these vortices matched measurement results and previous simulations, supporting the validity of the fluid dynamics calculations in the Purkinje fiber–considering model.
- Comparison of Q-value iso-surfaces showed that differences in left ventricular motion slightly influenced the flow field.

These results demonstrate that incorporating stimulus conduction via Purkinje fibers leads to different outcomes compared to the conventional model. This approach is essential for accurately reproducing left ventricular blood flow and understanding the causes of cardiac diseases. Future work will extend the simulation domain to the aorta.

References

1. WHO Homepage, <https://www.who.int/news-room/fact-sheets/detail/the-top-10-causes-of-death>, last accessed 2025/1/10
2. Dedè, L., Menghini, F., Quarteroni, A.: Computational fluid dynamics of blood flow in an idealized left human heart. *Int. J. Numer. Method Biomed. Eng.* 37(11), e3287 (2021). doi: 10.1002/cnm.3287
3. Xu, F., Kenjereš, S.: Numerical simulations of flow patterns in the human left ventricle model with a novel dynamic mesh morphing approach based on radial basis function. *Comput. Biol. Med.* 130, 104184 (2021). doi: 10.1016/j.compbimed.2020.104184
4. Schenkel, T., Malve, M., Reik, M., Markl, M., Jung, B., Oertel, H.: MRI-based CFD analysis of flow in a human left ventricle: methodology and application to a healthy heart. *Annals of biomedical engineering* 37, 503-515 (2009) . doi: 10.1007/s10439-008-9627-4
5. Cavero, I., Holzgrefe, H.: Remembering the canonical discoverers of the core components of the mammalian cardiac conduction system: Keith and Flack, Aschoff and Tawara, His, and Purkinje. *Advances in Physiology Education* 46(4), 549-579 (2022) . doi: 10.1152/advan.00072.2022
6. Strocchi, M., Gillette, K., Neic, A. et al.: Effect of scar and His–Purkinje and myocardium conduction on response to conduction system pacing. *Journal of cardiovascular electrophysiology* 34(4), 984-993 (2023) . doi: 10.1111/jce.15847
7. Norouzi, S., Goudarzi, T.: Effects of fiber orientation and the anisotropic behavior of the cardiac tissue on the simulated electrocardiogram. *Acta Mechanica* 233(10), 3881-3892 (2022) . doi: 10.1007/s00707-022-03286-4
8. Yamakawa, M., Takekawa, D., Matsuno, K., Asao, S.: Numerical simulation for a flow around body ejection using an axisymmetric unstructured moving grid method.

- Computational Thermal Sciences: An International Journal 4(3), 217-223 (2012) . doi: 10.1615/ComputThermalScien.2012004715
9. Asao, S., Matsuno, K., Yamakawa, M.: Simulations of a falling sphere with concentration in an infinite long pipe using a new moving mesh system. *Applied thermal engineering*, 72(1), 29-33 (2014). doi: 10.1016/j.applthermaleng.2014.06.059
 10. Yoon, S., Jameson, A.: Lower-upper symmetric-Gauss-Seidel method for the Euler and Navier-Stokes equations. *AIAA journal*, 26(9), 1025-1026 (1988) . doi: 10.2514/3.10007
 11. Van der Vorst, H. A.: Bi-CGSTAB: A fast and smoothly converging variant of Bi-CG for the solution of nonsymmetric linear systems. *SIAM Journal on scientific and Statistical Computing*, 13(2), 631-644 (1992) . doi: 10.1137/0913035
 12. Yamakawa, M., Kita, Y., Matsuno, K.: Domain decomposition method for unstructured meshes in an OpenMP computing environment. *Computers & Fluids* 45(1), 168-171 (2011) . doi: 10.1016/j.compfluid.2011.02.008
 13. Liang, F., Liu, H.: A closed-loop lumped parameter computational model for human cardiovascular system. *JSME International Journal Series C Mechanical Systems, Machine Elements and Manufacturing* 48(4), 484-493 (2005) . doi: 10.1299/jsmec.48.484
 14. Murata, K., Akagawa, E., Tanaka, T.: 2D Tissue Tracking Technique Demonstrates Attenuated Apical Endocardial Rotation in Patients with Dilated Cardiomyopathy, *MEDIX*, 46, 8-11 (2007)
 15. Durrer, D., Van Dam, R. T., Freud, G. E., Janse, M. J., Meijler, F. L., Arzbaecher, R. C.: Total excitation of the isolated human heart. *Circulation* 41(6), 899-912 (1970) . doi: 10.1161/01.CIR.41.6.899
 16. Elbrønd, V. S., Thomsen, M. B., Isaksen, J. L. et al.: Intramural Purkinje fibers facilitate rapid ventricular activation in the equine heart. *Acta Physiologica* 237(3), e13925 (2023) . doi: 10.1111/apha.13925
 17. Ito, Y., Nakahashi, K.: Surface triangulation for polygonal models based on CAD data. *Int. J. Numer Methods Fluids* 39(1), 75-96 (2002) . doi: 10.1002/fld.281
 18. Ito, Y.: Challenges in unstructured mesh generation for practical and efficient computational fluid dynamics simulations. *Computers & Fluids* 85, 47-52 (2013). doi: 10.1016/j.compfluid.2012.09.031
 19. Fantoni, C., Kawabata, M., Massaro, R. et al.: Right and left ventricular activation sequence in patients with heart failure and right bundle branch block: a detailed analysis using three-dimensional non-fluoroscopic electroanatomic mapping system. *Journal of cardiovascular electrophysiology* 16(2), 112-119 (2005). doi: 10.1046/j.1540-8167.2005.40777.x
 20. Kilner, P. J., Yang, G. Z., Wilkes, A. J., Mohiaddin, R. H., Firmin, D. N., Yacoub, M. H.: Asymmetric redirection of flow through the heart. *Nature* 404(6779), 759-761 (2000) . doi: 10.1038/35008075
 21. Kaur, H., Assadi, H., Alabed, S. et al.: Left ventricular blood flow kinetic energy assessment by 4D flow cardiovascular magnetic resonance: a systematic review of the clinical relevance. *J. Cardiovasc. Dev. Dis.* 7(3), 37 (2020) . doi: 10.3390/jcdd7030037